Accepted to Phys. Fluids 10.1063/5.0155675

A Precisive Calculation Methods of Volumetric and Hydraulic Efficiency of Centrifugal Pumps

Yu-Liang Zhang[1](张玉良), and Wen-Guang Li[2*](李文广)
1 School of Mechanical Engineering, Quzhou University, Quzhou, 324000, China
2 School of Engineering, University of Glasgow, Glasgow, G12 8QQ, UK
Email: Zhang002@sina.com(Yu-Liang Zhang), Wenguang.li@glasgow.ac.uk(Wen-Guang Li)
*The corresponding author

Abstract

This paper proposes a new method to calculate the volumetric efficiency and hydraulic efficiency of centrifugal pumps based on the principle of energy balance. Two efficiencies are calculated by means of a low specific speed centrifugal pump handling media with different viscosities at best efficiency points and are compared with that of two existing methods. The results manifest that the definition of two efficiencies in the present paper is more precisive and sensitive to the change of liquid viscosity.

Keywords: centrifugal pump; volumetric efficiency; hydraulic efficiency; hydraulic loss; Reynolds number; viscosity

Accepted to Phys. Fluids 10.1063/5.0155675

1 Introduction

Centrifugal pumps are widely used to deliver various kinds of fluids. The total loss of centrifugal pumps includes mechanical, volumetric, and hydraulic losses [1, 2]. Wherein the mechanical losses mainly are composed of the disc friction loss and mechanical losses in shaft seals and bearings [3]. The volumetric loss acts as a leakage through the clearance of the wear-ring in the front chamber [4]. If there are balance holes in the rear chamber, the volumetric loss would be doubled [5]. Hydraulic losses are present in any flow passages in the pump. In the early numerical calculations, the flow in the front and rear chambers often is not considered in order to simplify the calculation. Such that, the leakage needs to be corrected by means of the empirical formula [6]. Nowadays, the flow in front and rear chambers are often calculated together with the flow in impeller and volute, and the magnitude of the leakage is calculated directly through numerical calculations [7]. The hydraulic loss through an arbitrary flow-through component is often determined by the differential total pressure in a rotating or stationary reference frame system between the inlet and outlet of the component. In recent years, the entropy production method has also been widely used to predict the local hydraulic losses in the pump [8-12].

For a given centrifugal pump, the total loss is certain in magnitude, and if the calculation of one loss is incorrect, then the calculation of the other one or two losses is also incorrect. For a low specific speed centrifugal pump, the total loss would be greater, and the total efficiency would be lower, so the above problem would be more prominent. In this paper, we would analyze and propose the calculation method for each loss from the principle of energy balance in the pump. Finally, the precise calculation methods of the volumetric efficiency and hydraulic efficiency would be proposed. These losses are calculated accurately to provide the necessary support and efforts for hydraulic optimization and structural optimization.

2 Proposal of new method

A sketch of the liquid flow in the meridional plane of impeller in a centrifugal pump is illustrated in Fig. 1, where Q is the liquid flow rate across the pump inlet or outlet, q is the leakage flow rate through the front chamber and the gap in the wear-ring, Q_t represents the theoretical flow rate through the impeller, obviously, $Q_t = Q + q$.

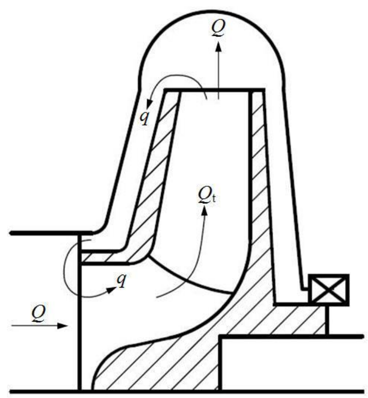

Fig. 1 Sketch of liquid flow in the meridional plane of impeller in a centrifugal pump

The diagram of energy balance in a centrifugal pump is indicated in Fig. 2, where P is the power input of the pump, i.e., shaft-power, P_o is the power output, P_o=ρgQH, H is the pump head, ρ is the liquid density, g is the acceleration due to the gravity. In the figure H_t is the impeller theoretical head, P_m is the disc friction loss power of the impeller, P_{sb} is the loss power in the shaft seals and bearings. P_v is the volumetric loss power, $P_v = \rho gq(H_t - h_i)$, h_i is the hydraulic loss in the impeller; P_{hi} denotes the hydraulic loss power of the impeller, $P_{hi} = \rho gQ_t h_i$, P_{hV} represents the hydraulic loss power in the volute, $P_{hV} = \rho gQh_V$, h_V is the hydraulic loss in the volute, h indicates the total hydraulic loss in the pump, $h = h_i + h_V$.

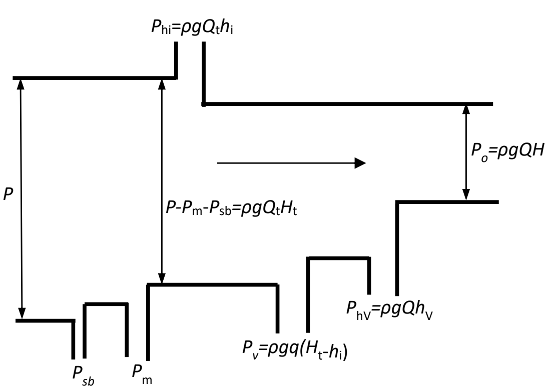

Fig. 2 Diagram of energy balance in a centrifugal pump

Referring to Fig. 2, we can define the mechanical efficiency, volumetric efficiency and hydraulic efficiency according to the mechanical loss power, volumetric loss power and hydraulic loss power, respectively. The three efficiencies are calculated by the following expressions:

Mechanical efficiency

$$\eta_m = \frac{P-P_m-P_{sb}}{P} \tag{1}$$

Volumetric efficiency

$$\eta_v = \frac{P-P_m-P_{sb}-P_v}{P-P_m-P_{sb}} = \frac{P-P_m-P_{sb}-\rho gq(H_t-h_i)}{P-P_m-P_{sb}} \tag{2}$$

Hydraulic efficiency

$$\eta_h = \frac{P-P_m-P_{sb}-P_v-P_{hi}-P_{hv}}{P-P_m-P_{sb}-P_v} = \frac{P-P_m-\rho gq(H_t-h_i)-\rho gQ_t h_i-\rho gQh_v}{P-P_m-\rho gq(H_t-h_i)} = \frac{P-P_m-\rho gqH_t-\rho gQh}{P-P_m-P_{sb}-\rho gq(H_t-h_i)} \tag{3}$$

Overall efficiency

$$\eta = \frac{P-P_m-P_{sb}-P_v-P_{hi}-P_{hv}}{P} = \left(\frac{P-P_m-P_{sb}}{P}\right)\left(\frac{P-P_m-P_{sb}-P_v}{P-P_m-P_{sb}}\right)\left(\frac{P-P_m-P_{sb}-P_v-P_{hi}-P_{hv}}{P-P_m-P_{sb}-P_v}\right) = \eta_m\eta_v\eta_h \tag{4}$$

In the literature, the mechanical efficiency definition is identical, but the hydraulic efficiency and volumetric efficiency definitions are different. For example, there is an energy balance diagram in a centrifugal pump as shown in Fig. 3 was proposed in [10].

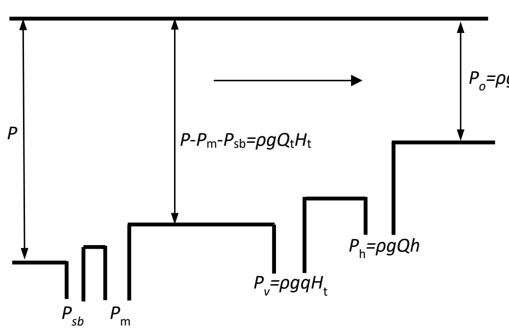

Fig. 3 Diagram of energy balance in a centrifugal pump proposed by Stepanoff in [13]

Stepanoff in [13] suggests the hydraulic efficiency and volumetric efficiency should be defined as:

$$\eta_v = \frac{P-P_m-P_{sb}-P_v}{P-P_m-P_{sb}} = \frac{\rho gQ_tH_t-\rho gqH_t}{\rho gQ_tH_t} = \frac{Q}{Q_t} = 1-\frac{q}{Q_t} \tag{5}$$

where Q_t=$Q+q$, $P-P_m-P_{sb}$=$\rho g Q_t H_t$, P_v=$\rho g q H_t$, and

$$\eta_h=\frac{P-P_m-P_{sb}-P_v-P_h}{P-P_m-P_{sb}-P_v}=\frac{\rho g Q_t H_t-\rho g q H_t-\rho g Q h}{\rho g Q_t H_t-\rho g q H_t}=\frac{H}{H_t}=1-\frac{h}{H_t} \tag{6}$$

where P_h=$\rho g Q h$. Then the overall efficiency is written as:

$$\eta=\left(\frac{P-P_m-P_{sb}}{P}\right)\left(\frac{P-P_m-P_{sb}-P_v}{P-P_m-P_{sb}}\right)\left(\frac{P-P_m-P_{sb}-P_v-P_h}{P-P_m-P_{sb}-P_v}\right)=\eta_m\eta_v\eta_h \tag{7}$$

Additionally, based on the diagram of energy balance in Fig. 2, the volumetric efficiency, hydraulic efficiency, and overall efficiency are defined as in [14]:

$$\eta_v=\frac{P-P_v}{P}=\frac{P-\rho g q(H_t-h_i)}{P} \tag{8}$$

and

$$\eta_h=\frac{P-P_{hi}-P_{hv}}{P}=\frac{P-\rho g Q h-\rho g q h_i}{P} \tag{9}$$

but the overall efficiency is defined as:

$$\eta=\frac{P-P_m-P_{sb}-P_v-P_{hi}-P_{hv}}{P}=\eta_m+\eta_v+\eta_h-2 \tag{10}$$

3 Comparison and discussion

To clarify which set of definitions expressed by Eqs. (1)-(10) to be proper and reasonable, a single-stage, single-suction, hot-oil centrifugal pump of 65Y60 was selected and its mechanical efficiency, volumetric efficiency and hydraulic efficiency at best efficiency point (BEP) were calculated when handling water and viscous oil, respectively. The cross-sectional views of the pump and impeller are illustrated in Fig. 4. The pump has been employed to investigate effects of viscosity [15], number of blades [16] and blade exit angle [17] on the pump performance, respectively.

(a)

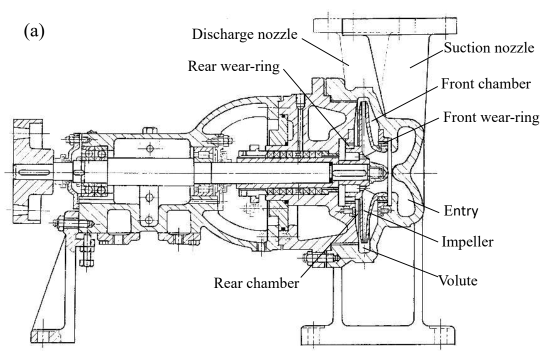

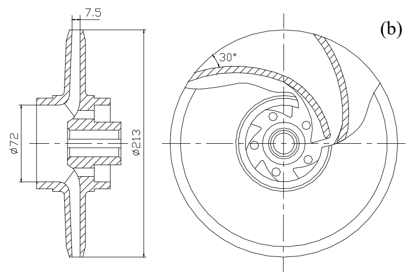

Fig. 4 Cross-sectional view of the pump (a), impeller style and its major dimensions (b)

The performance specifications of the pump are as follows: flow rate Q=25 m^3/h, head H=60 m, rotating speed n=2950 r/min, and the specific speed n_s=41.6. The geometrical parameters of the pump, impeller and volute are listed in Table 1 and density and kinematic viscosity of water and oil are provided in Table 2. The hydraulic, volumetric and disc friction losses were analysed at the known flow rate measured at BEP listed in Table 2 by using hydraulic loss, leakage flow and disc friction models presented in Appendix.

Table 1 Geometrical parameters of the impeller, volute, wear-ring and side chamber of the pump

Item	Paremeter	Value	Remark
Suction nozzle	Diameter d_s(mm)	65	
Impeller	Inlet diameter, D_1(mm)	62	
	Outlet diameter, D_2(mm)	213	
	Inlet width of blade, b_1(mm)	16	
	Outlet width of blade, b_2(mm)	7.5	
	Number of blades, Z	5	
	Blade entrance angle, β_1(°)	25	
	Blade exit angle, β_2(°)	30	
	Thickness of blade at outlet, s_2(mm)	5	
	Roughness inside impeller, Ra_i(μm)	25	Painted
	Roughness outside impeller, Ra_o(μm)	6.3	Painted
Volute	Width, b_3(mm)	16	
	Base circle diameter, D_3(mm)	240	
	Area of throat, F_8(cm^2)	6.42	
	Circumferential angle of tongue, φ_0(°)	36	
	Discharge nozzle length, L_{89}(mm)	250	
	Discharge nozzle diameter, D_9(mm)	60	
	Roughness inside volute, Ra_V(μm)	25	Painted
	Roughness inside nozzle, Ra_d(μm)	25	Painted

Wear-ring	Front	Dimeter, D_{wf}(mm)	100	
		Radial gap, b_{wf}(mm)	0.25	
		Gap length, l_{wf}(mm)	15	
	Rear	Dimeter, D_{wr}(mm)	100	
		Radial gap, b_{wr}(mm)	0.25	
		Gap length, l_{wr}(mm)	15	
Side chamber	Front	Width, t_f(mm)	7	
	Rear	Width, t_r(mm)	7	
Balance hole	Diameter of hole, d_b(mm)		8	
	Number of holes, Z_b		5	

Table 2 Kinematic viscosity of water and machine oil, pump flow rate measured at BEP

Parameter	Water	Machine oil						
ν(cSt)	1	29	45	75	99	134	188	255
ρ(kg/m^3)	1000	870.8	877.2	883.0	885.6	888.2	890.9	892.9
Q_{BEP}(m^3/h)	32.8	32.5	32.4	32.4	32.5	32.5	32.0	29.0

The pump head, hydraulic power, and overall efficiency at BEP predicted by using the models in Appendix are illustrated and compared with the experimental data given by [15-17] in Fig. 5. The mean errors of the head, hydraulic power and overall efficiency between prediction and experiment are 1.47±1.50%, 2.62±1.97%, and 2.09±1.68%, respectively. This fact suggests that the models used in the paper are proper and reasonable. Note that the sharp variation in the head, hydraulic power and overall efficiency curves indicate a transition from hydraulically rough regime to hydraulically smooth regime of boundary layer flow inside the flow passages and over the casing walls and impeller outside surfaces due to increase of liquid viscosity.

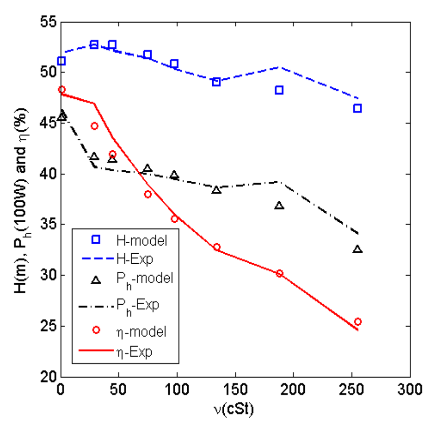

Fig. 5 Head, hydraulic power and overall efficiency at BEP predicted by using the models in Appendix and compared with the corresponding experimental data in [15-17]

The hydraulic, volumetric and disc friction loss powers were predicted by the flow models in the Appendix at BEP, then the hydraulic, volumetric, mechanical and overall efficiencies were calculated by using Eqs. (1)-(10), respectively. These efficiencies are shown as a function of liquid viscosity and compared among three definition methods in Fig. 6. Since the definition of mechanical and overall efficiencies is identical in the three methods, the two efficiencies remain unchanged and overlapped across the three methods. Fig. 6(a) does demonstrate that fact.

The volumetric efficiencies calculated by the three methods rise with increasing liquid viscosity, further, the magnitude of the efficiency defined by Yang and Zhang [14] is the highest, the efficiency defined by Stepanoff [13] is the lowest, while the efficiency defined in the present paper is in between at a given viscosity.

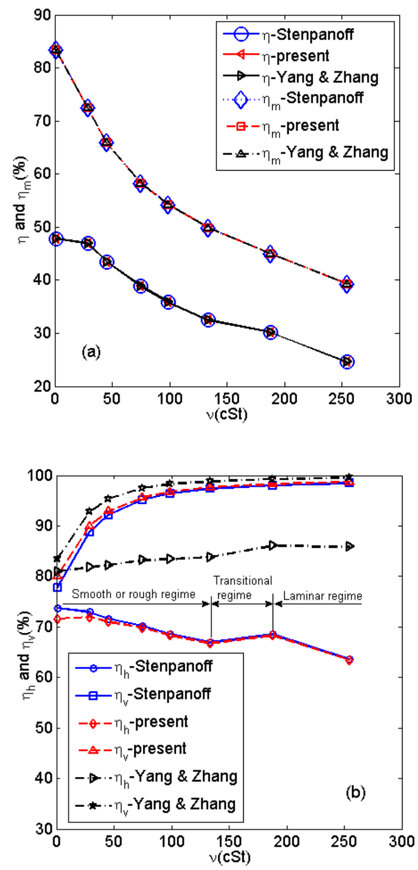

Fig. 6 Overall, mechanical, hydraulic , and volumetric efficiencies at BEP are plotted against liquid

viscosity, those efficiencies were calculated by using Eqs. (1)-(10) based on the hydraulic, volumetric and disc friction losses predicted with the flow models in the Appendix, (a) overall efficiency η and mechanical efficiency η_m, (b) hydraulic efficiency η_h and volumetric efficiency η_v

The hydraulic efficiency given by Yang and Zhang [14] is the highest but also rises slightly with increasing viscosity. This variation trend is irrational because the increasing viscosity usually leads to an increase in hydraulic losses in the impeller and volute (see Fig. 7) and subsequently deteriorates the hydraulic efficiency. The hydraulic efficiency in the present paper is larger than that after Stepanoff [13] when the viscosity is lower than 45cSt. Beyond that viscosity they share nearly the same value. Further, the two efficiencies decline with increasing viscosity. This trend reflects a matter of fact that the hydraulic losses increase with increasing viscosity as shown in Fig. 7.

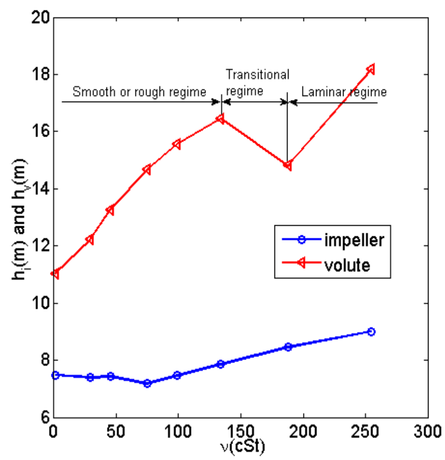

Fig. 7 Predicted hydraulic losses in the impeller and volute are plotted as a function of liquid viscosity

The volumetric efficiency η_v defined in Eq. (2) in the present paper has considered the hydraulic loss across the impeller h_i. This means that the volumetric loss across the wear-rings is driven by the head H_t-h_i rather than the impeller theoretical head H_t used in Eq. (5). By using the relationship: $P-P_m-P_{sb}$=$\rho g Q_t H_t$, Eq. (2) can be simplified to the following form:

$$\eta_v=\frac{\rho g Q_t H_t-\rho g q(H_t-h_i)}{\rho g Q_t H_t}=1-\left(\frac{h_i}{H_t}\right)\left(\frac{q}{Q_t}\right) \tag{11}$$

If h_i is ignored, Eq. (11) is identical to Eq. (5). Otherwise, the η_v in Eq. (11) is higher than that in Eq. (5). The head H_t-h_i was adapted in the volumetric efficiency η_v by Yang and Zhang in [11], the power input or shaft power can be written as: P=$\rho g Q_t H_t+P_m+P_{sb}$. Thus, Eq. (8) can be reduced to:

$$\eta_v = 1 - \left(\frac{1}{1+\frac{P_m+P_{sb}}{\rho g Q_t H_t}}\right)\left(\frac{q}{Q_t}\right) + \left(\frac{\frac{h_i}{H_t}}{1+\frac{P_m+P_{sb}}{\rho g Q_t H_t}}\right)\left(\frac{q}{Q_t}\right) \quad (12)$$

Based on Eqs. (8), (11), and (12), the η_v defined in Eq. (8) is the largest, and the η_v defined in Eq. (5) is the smallest, but the η_v defined in Eq. (2) is in between them at a given liquid viscosity. With increasing viscosity, the η_v approaches 100%, the volumetric efficiencies given by three types of definition show a less difference.

The hydraulic efficiency η_h defined by Eqs. (3) and (6) is similar in form, while the corresponding volumetric loss power P_v formulas are different, therefore, the hydraulic efficiency η_h is different, especially at a low viscosity. With $P - P_m + P_{sb}$=$\rho g Q_t H_t$, Eq. (3) can be rewritten as:

$$\eta_h = 1 - \left[\frac{h}{H_t}\frac{1}{\left(1-\frac{h_i}{H_t}\right)\frac{Q}{Q_t}+\frac{h_i}{H_t}} - \frac{h_v}{H_t}\frac{1}{\left(1-\frac{h_i}{H_t}\right)\frac{Q}{Q_t}+\frac{h_i}{H_t}}\frac{q}{Q_t}\right] \quad (13)$$

Let P=$\rho g Q_t H_t + P_m + P_{sb}$ once again, Eq. (9) can be cast in the following form:

$$\eta_h = 1 - \left[\frac{h}{H_t}\frac{1}{1+\frac{P_m+P_{sb}}{\rho g Q_t H_t}}\frac{Q}{Q_t} - \frac{h_v}{H_t}\frac{1}{1+\frac{P_m+P_{sb}}{\rho g Q_t H_t}}\frac{q}{Q_t}\right] \quad (14)$$

Although we know the fact of 0<$\left(1-\frac{h_i}{H_t}\right)\frac{Q}{Q_t}+\frac{h_i}{H_t}$<1 and $1+\frac{P_m+P_{sb}}{\rho g Q_t H_t}$>1, it is very hard to compare Eqs. (9), (13) and (14) in magnitude. Hence, the h/H_t in Eq. (9), difference of the last two terms, and last one term in Eqs. (13) and (14) are plotted as a function of liquid viscosity in Fig. 8. It is suggested that the last one term is much lower (<0.04) than the second term in in Eqs. (13) and (14), especially at ν ≥50cSt, and can be negligible.

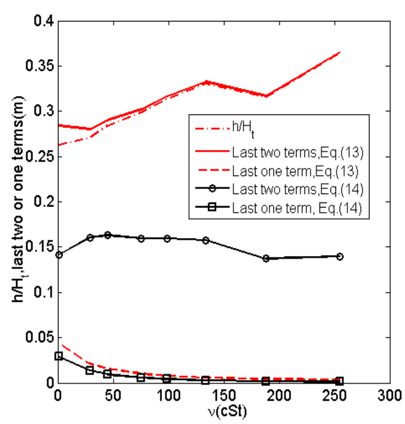

Fig. 8 h/H_t in Eq. (9), last two terms and last one term in Eqs. (13) and (14) are plotted as a functions of liquid viscosity, the last two terms in the figure represent their differences in the square brackets in the equations

The difference of the last two term in Eq. (13) is slightly larger the h/H_t in Eq. (9), and the difference and h/H_ty rises steadily with increasing viscosity. The difference of the last two terms in Eq. (14) is about more half less than the h/H_t in Eq. (9), but also insensitive to the change of liquid viscosity. This effect may be attributed the dramatic augmentation of disc friction loss $\frac{P_m+P_{sb}}{\rho g Q_t H_t}$ with increasing viscosity. The curves in Fig. 9 explain the variation trend of the hydraulic efficiencies in Fig. 8 exactly.

According to Eqs. (12) and (14), the disc friction loss has been involved directly into the formulas of volumetric and hydraulic efficiencies. As a result, the disc friction loss not only affects mechanical efficiency, but also alters volumetric and hydraulic efficiencies. The definition of the mechanical, volumetric and hydraulic efficiencies proposed by Yang and Zhang [14] appears imperfect and misleading. The hydraulic efficiency fails to reflect the change of liquid viscosity.

In the definition of volumetric efficiency by Stepanoff [13], the leakage flow is driven by the impeller theoretical head H_t, resulting in the volumetric loss power P_v=$\rho g q H_t$. In fact, the liquid must experience the hydraulic loss h_i across an impeller, thus the leakage flow should be driven by the impeller actual head H_t-h_i, and the corresponding volumetric loss power P_v=$\rho g q(H_t - h_i)$. In the present paper, it is considered that the leakage flow is driven by the impeller actual head H_t-h_i. As a result, the volumetric efficiency calculated by using the formula proposed by the present paper is more precisive and sensitive to the change of liquid viscosity than that by Stepanoff [13]. Naturally, the hydraulic efficiency calculated by means of the formula defined in the present paper is also more precisive and sensitive to the change of liquid viscosity than the hydraulic efficiency by Stepanoff in [13] since the formulas for the overall efficiency and mechanical efficiency in the present paper are the same as those in [13].

4 Discussion

It is shown that the pump head, hydraulic power and efficiency in Fig. 5 and the hydraulic efficiency In Fig. 6 (b) exhibit a notable variation at ν=29, 134, 188cSt. This effect is related to flow regime transition in the pump. Based on Fig. 7 the hydraulic loss the volute is dominant compared with the loss in the impeller. Thus, the effect should be attributed to the flow regime transition in the volute. The skin friction factor of the flow in the volute λ_V calculated by using the formulas in Appendix is plotted as a function of the Reynolds number of the volute Re_V in Fig. 9. In the figure, there are transitions from hydraulically rough regime to hydraulically smooth regime at ν=29cSt and from hydraulically smooth regime to transitional regime at ν=134cSt as well as from transitional regime to laminar regime at ν=188cSt, respectively. There is a considerable reduction in friction factor at ν=188cSt when the boundary layer flow in the volute changes into the laminar regime from the transitional regime due to the increasing viscosity. Accordingly, the hydraulic loss in the volute reduces significantly in Fig.7; thus, the overall efficiency in Fig. 5 and the hydraulic efficiency in Fig. 6(b) rise.

Since the predicted overall efficiency is higher than the experimental overall efficiency as shown in Fig. 5, the friction factor is underestimated in the transitional regime here. In fact, there is no empirical correlation for the transitional regime between the laminar regime and the hydraulic smooth regime in the literature. It has to be assumed that the laminar regime occurs suddenly at Re_V=2300 in the paper. As a result, the friction factor drops off sharply when the boundary layer flow enters the laminar regime from the transitional regime. Hopefully, this limitation can be removed when the empirical correlation for the transitional regime is available in the future.

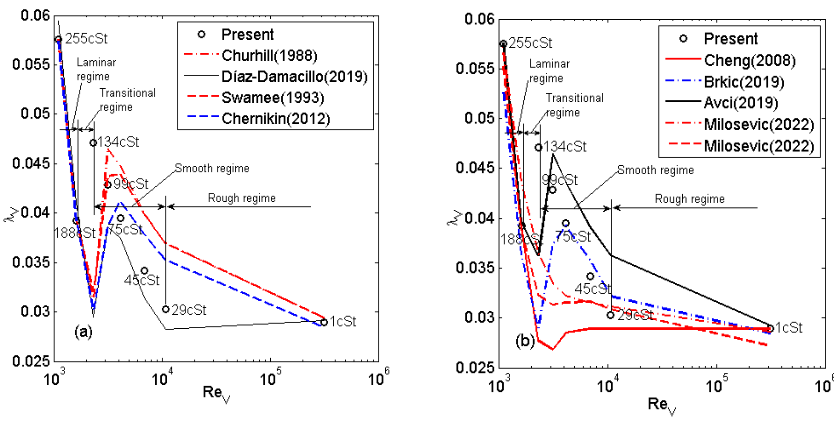

Fig. 9 Skin friction factors of the flow in the volute λ_V calculated by the formulas in Appendix and the other unified empirical formulas in [31] are plotted against the Reynolds number of the volute Re_V, (a) for the correlations proposed by Churhill(1988), Diaz-Damacillo (2019), Swamee (1993) and Chernikin (2012), respectively; (b) for the correlations proposed by Cheng(2008), Brkic (2019), Avci (2019) and Milosevic (2022), respectively

To compare the empirical corelations for friction factor, the friction factor in the volute was calculated the unified empirical formulas for all the boundary layer flow regime presented in [31] and included in Fig. 9. The unified formulas proposed by Cheng (2009), Milosevic (2022) failed to predict the hydraulically smooth regime. The other unified empirical formulas predict the larimar regime starts at ν=134cSt, but also overestimate the λ_V value in the hydraulically smooth regime. Even though a unified formula can simplify programming, these unified empirical formulas are not adopted in the paper because of their unsatisfactory performance in prediction.

The paper is subject to a few limitations. First, the dimensionless mean rotating angular velocity coefficients of the liquid in the side chambers are valid only at zero leakage flow rate. The influence of leakage flow rate on the coefficients needs to be modelled analytically in the future. Second, the proposed hydraulic, volumetric and disc friction models are limited to BEP, and the models at part- and over-load points need to be developed in the future. Third, the models are applied to only one centrifugal pump due to the limitation in experimental data. It is hopeful that there are more experimental data on centrifugal pumps with different specific speeds. In the future, the volumetric and hydraulic efficiencies calculated by the proposed definition method may be compared with the results obtained by a fully three-dimensional CFD simulations of flow field in a centrifugal pump at various viscosities.

5 Conclusion

The proposed method in this paper has more obvious physical meaning, such that it is more reasonable and has better accuracy. Compared with the definition of volumetric and hydraulic efficiencies by Stepanoff, the definitions in the present paper is more precisive, and sensitive to the change of liquid viscosity. The hydraulic loss in the volute is larger than that in the impeller. Although the existing unified empirical formulas could simplify programming, it is not able to accurately reflect the skin friction factor. With increasing viscosity, the volumetric efficiency gradually rises and approaches to 100%, the volumetric efficiencies among three definitions show a less difference.

Acknowledgement

The research was financially supported by the "Pioneer" and "Leading Goose" R&D Program of Zhejiang (Grant No. 2022C03170), Science and Technology Project of Quzhou (Grant No.2022K98).

Declaration of conflicting interests

The author(s) declared no potential conflicts of interest with respect to the research, authorship, and/or publication of this article.

Data Accessibility

The data used to support the findings of this study are available from the corresponding author upon request.

ORCID iD

Yu-Liang Zhang: https://orcid.org/0000-0003-3249-5629.

Wenguang Li: https://orcid.org/0000-0003-3209-0728.

Nomenclature

b width of blade, mm

b_3 width of volute, mm

b_w clearance of the wear-ring, mm

C_M torque coefficient due to disc friction

D diameter, mm

D_3 diameter of circle tangential to volute tongue tip, mm

D_8 equivalent diameter of volute throat, mm

D_{89} mean diameter of D_8 and D_9, mm

D_9 diameter of nozzle exit, mm

D_h hydraulic diameter, m

D_w diameter of the wear-rings, mm

d_b diameter of balance holes, mm

F_0 cross-sectional area of section 0-0, m^2

F_2 exit area of impeller, m^2

F_8 throat area of volute, m^2

F_9 cross-sectional area of nozzle exit, m^2

F_m mean area of F_0 and F_8 of the volute body, m^2

F_w cross-sectional area of the clearance of the wear-rings, m^2

f_{geo} impeller shape factor on disk friction loss

f_L leakage flow rate influencing factor on torque coefficient

g acceleration due to gravity, m/s^2

h total hydraulic loss, m

h_l total hydraulic loss, m

h_{id} expansion loss in impeller, m

h_{ie} mixing loss behind impeller, m

h_{if} skin friction loss in impeller, m

h_V total hydraulic loss in volute, m

h_{Vde} expansion loss in nozzle, m

h_{Vdf} skin friction loss in nozzle, m

h_{Vf} skin friction loss in spiral body of volute, m

H pump head, m

H_t theoretical head of impeller, m

H_w pressure difference across the wear-rings, m

k_s equivalent sand roughness of wetted wall, m

k_{sifc}, k_{sirc} critical equivalent sand roughness on the impeller shroud and hub, m

L_i blade length, cm

L_{89} length of discharge nozzle, mm

L_V length of spiral body of volute, mm

n pump rotating speed, r/min

n_s specific speed of pump, $n_s = \frac{3.65n[r/min]\sqrt{Q[m^3/s]}}{H[m]^{3/4}}$

P shaft-power of pump, W

P_h pump hydraulic power, W

P_m disc friction loss power of the impeller, W

P_{sb} mechanical loss power in shaft seals and bearings, W

Q pump flow rate, m^3/h

Q_t theoretical flow rate through impeller, m^3/h

q leakage flow rate through the clearance in the wear-rings, m^3/h

R radius, mm

Ra Roughness of wetted surface, mm

Re Reynolds number

Re_{wfc}, Re_{wrc} critical Reynolds numbers determining low regimes in the clearance of the wear-rings

R_w radius of wear-rings on impeller

s metal thickness of blade, mm

t distance between casing and impeller shroud or hub, mm

T_u turbulent intensity of boundary layer

u_w wear-ring rotational speed, m/s

V_3 mean velocity in volute, m/s

V_{89} mean velocity through area of $\pi D_{89}^2/4$, m/s

V_9 mean velocity through nozzle exit, m/s

V_m meridional velocity, m/s

V_u circumferential absolute velocity, m/s

W mean relative velocity of W_1 and W_2, m/s

W_1 relative velocity at entrance of impeller, m/s

W_2 relative velocity at exit of impeller, m/s

$W_{2\infty}$ relative velocity at the exit of impeller with infinite number of blades, m/s

Greek

β blade angle, deg

δ thickness of sub-laminar layer, m

ΔV_{u2} slip velocity at impeller outlet, m/s

η total efficiency

η_h hydraulic efficiency

η_V volumetric efficiency

η_m mechanical efficiency

θ equivalent diffusion angle of impeller passage or discharge nozzle, deg

κ dimensionless mean rotating angular velocity coefficient of the liquid in a side chamber, rad/s

λ skin friction factor

ν kinematic viscosity of fluid, cSt (mm^2/s)

ξ expansion loss coefficient

ξ_0 expansion loss coefficient when $Re \geq 4\times 10^5$

ρ liquid density, kg/m^3

σ slip factor

Z number of blades

Z_b number of balance holes

ϕ_0 circumferential angle of tongue of volute, deg

ψ blockage factor of blade

ω angular speed of impeller, rad/s

ω_f angular speed of liquid in a side chamber, rad/s

Subscription

1 inlet

2 outlet

c casing

cr critical

d discharge nozzle

f front

i impeller

r rear

V volute

Abbreviation

BEP best efficiency point

CFD computational fluid dynamics

Appendix Hydraulic, volumetric and disc friction loss models

The hydraulic, volumetric and disc friction loss models are essential in determination of the hydraulic, volumetric and mechanical efficiencies defined in Section 2. The hydraulic and disc friction loss models are associated with the previous publication [17] but updated with stuffings. For instance, the slip factor was replaced with the well-known Weisner's formula, effects of rotating angular speed of liquid in the side chambers, roughness of the inside surface and impeller outside were taken into account. A volumetric loss model for the leakage flow across the wear-rings and balance holes into the impeller entrance was developed. The rotating angular speed of liquid in the side chambers and roughness of the inside surface and impeller were included in the model, too.

A1 Hydraulic loss model

The flow of liquid in a centrifugal pump is supposed to be one-dimensional (1D), steady, either laminar or turbulent. This assumption suggests that the complex liquid flow in the pump can be represented by the simple 1D flow on the mean streamline in the impeller and the mid-span plane in the volute, respectively. The construction of the pump 65Y60 as shown in Fig. 4 and the velocity triangles at the inlet and outlet of the impeller are sketched in Fig. A1. It is assumed that the liquid has no pre-swirl at BEP. Based on the Euler's equation for turbomachinery, the theoretical head generated by the impeller is calculated by [18]:

$$H_t = \frac{u_2 V_{u2}}{g},\ V_{u2} = (1-\sigma)u_2 - \frac{V_{m2}}{\tan\beta_2},\ V_{m2} = \frac{Q_t}{\psi_2 F_2} \tag{A1}$$

where H_t is the theoretical head of the impeller, u_2 is the impeller peripheral speed, u_2=$R_2\omega$, R_2 is the impeller radius, R_2=0.5D_2, D_2 is the impeller diameter, ω is the impeller rotational angular speed, $\omega = \pi n/30$, n is the impeller rotational speed, V_{u2} and V_{m2} are the circumferential and meridional components of absolute velocity of liquid at the impeller outlet, respectively, Q_{th} is the liquid volumetric flow rate through the impeller, F_2 is the area of the impeller outlet, $F_2=\psi_2\pi D_2 b_2$, ψ_2 is the blade blockage factor at the outlet, $\psi_2=1-Z\,s_2\sin\beta_2/\pi D_2$, Z is the number of blades, s_2 is the metal thickness of blade at the impeller outlet, β_2 is the blade exit angle, σ is the Weisner's slip factor, and defined and expressed by the following empirical formulas [19]:

$$\sigma=\frac{\Delta V_{u2}}{u_2}=\frac{\sqrt{\sin\beta_2}}{Z^{0.7}} \tag{A2}$$

If the hydraulic loss in the pump h is known at BEP, the pump head H will be calculated from the impeller theoretical head H_t by:

$$H=H_t-h \tag{A3}$$

The liquid velocity in the side-entry of the pump shown in Fig.5a is slower than the velocities in the impeller and volute, hence the hydraulic loss in the entry is neglected. The angles of attack of the flow to the leading edge of blades of the impeller and the tongue of the volute are the smallest at BEP, the corresponding shock losses at the leading edge are minimal, thus ignored in the paper. This means that the liquid experiences skin friction and diffusion losses in the impeller.

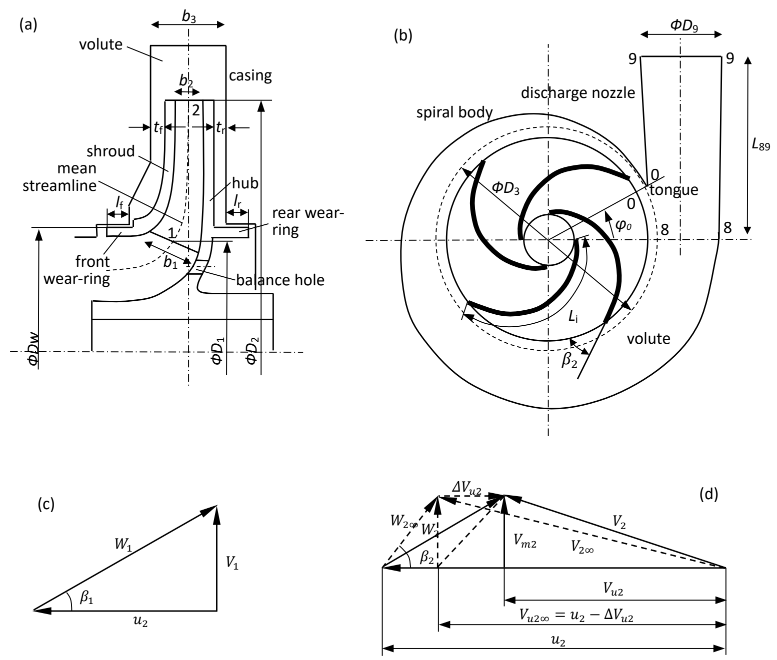

Fig. A1 Sketch of the pump 65Y60 shown in Fig. 5, (a) meridional view, (b) mid-span view, (c) velocity triangle at point 1 of inlet, (d) velocity triangle at point 2 of outlet, subscript ∞ indicates the situation where the number of blades is infinite

In the volute the liquid suffers from the skin friction loss in the spiral body as well as skin friction and diffusion losses in the discharge nozzle. Additionally, a mixing loss takes place on the interface between the impeller exit and the volute inlet. The complicated flow passages in the impeller and volute are considered as straight circular pipes by using the hydraulic diameter and length of the passages, and the skin friction coefficients in the pipes are employed to estimate the friction loss in the passages.

The hydraulic losses in the impeller are composed of the skin friction and diffusion losses. The friction loss is calculated by the following expression:

$$h_{if} = \lambda \frac{L_i}{D_{hi}} \frac{W^2}{2g} \tag{A4}$$

where L_i is the blade length along the mean streamline, and it is related to the blade exit angle β_2 of the impeller in the following expression:

$$L_i = 0.0033\beta_2^2 - 0.4567\beta_2 + 27.5 \ \text{(cm)} \tag{A5}$$

W is the mean relative velocity of the liquid in the impeller passages, and estimated by using the relative velocities at the impeller inlet and outlet in the following manner:

$$W = (W_1 + W_2)/2,\ W_1 = \sqrt{u_1^2 + V_1^2},\ W_2 = \sqrt{(u_2 - V_{u2})^2 + V_{m2}^2} \tag{A6}$$

where u_1 is the peripheral speed at the inlet of the impeller, u_1=$R_1\omega$, R_1 is the impeller inlet radius, R_1=0.5D_1, D_1 is the impeller inlet diameter, V_1 is the absolute velocity of the liquid at the inlet of the impeller, $V_1 = Q_{th}/F_1$, F_1=$\psi_1 \pi D_1 b_1$, ψ_1 is the blade blockage factor at the inlet, $\psi_1 = 1 - Z\, s_1 \sin\beta_1/\pi D_1$, s_1 is the metal thickness of blade at the impeller inlet. The hydraulic diameter D_{hi} is estimated by the expression:

$$D_{hi} = \frac{1}{2}\left(\frac{\frac{4\pi D_1 b_1}{Z}}{2b_1 + \frac{2\pi D_1}{Z}} + \frac{\frac{4\pi D_2 b_2}{Z}}{2b_2 + \frac{2\pi D_2}{Z}}\right) \tag{A7}$$

further, Eq. (A7) can be simplified to the following formula:

$$D_{hi} = \frac{D_1 b}{Z b_1 + \pi D_1} + \frac{D_2 b_2}{Z b_2 + \pi D_2} \tag{A8}$$

The diffusion loss in the impellers can be calculated by using the following equation:

$$h_{id} = \xi \frac{W_1^2}{2g} \tag{A9}$$

where the diffusion coefficient ξ is a function of the equivalent expansion angle of the impeller flow passages θ_i, and calculated by:

$$\theta_i = 2\tan^{-1}\left[\frac{\pi(D_2 - D_1)}{2ZL_i}\right] \tag{A10}$$

Three kinds of hydraulic loss exist in the volute. One is the skin friction loss in the spiral body, the other two are the friction and diffusion losses in the discharge nozzle. The friction loss at the wall of the spiral body is estimated by the expression:

$$h_{Vf} = \lambda \frac{L_V}{D_{hV}} \frac{V_3^2}{2g} \tag{A11}$$

The hydraulic diameter D_{hV} is determined by the mean cross-section area of the volute and written as:

$$D_{hV} = \frac{4F_m}{b_3 + 2F_m/b_3} \tag{A12}$$

The mean cross-section area F_m is calculated by the areas F_0 and F_8 of the cross-sections 0-0 and 8-8, expressed as:

$$F_m = \frac{1}{2}(F_0 + F_8) \tag{A13}$$

where the area $F_0 = 0.5(D_3 - D_2)b_3$. The mean velocity of liquid V_3 in the volute is calculated by:

$$V_3 = Q(1 - \phi_0/360)/F_8 \tag{A14}$$

where Q is the ump flow rate, ϕ_0 is the initial circumferential angle. The length of the spiral body L_V is estimated by using the formula:

$$L_V = \pi D_3(1 - \phi_0/360) \tag{A15}$$

The skin friction loss in the discharge nozzle is calculated by means of the expression:

$$h_{Vdf} = \lambda \frac{L_{89}}{D_{89}} \frac{V_{89}^2}{2g} \tag{A16}$$

where L_{89} is the length of the discharge nozzle, D_{89} is the mean diameter of the nozzle is estimated by the equivalent diameter of the section 8-8 D_8 and the outlet diameter of the nozzle D_9:

$$D_{89} = \frac{1}{2}(D_8 + D_9),\ D_8 = \sqrt{4F_8/\pi} \tag{A17}$$

The velocity of the liquid in the pipe with a diameter of D_{89} is calculated by:

$$V_{89} = Q/F_{89} \tag{A18}$$

where F_{89} is the area of a pie with the diameter D_{89}, $F_{89} = \pi D_{89}^2/4$. The diffusion loss in the discharge nozzle is given by the following equation:

$$h_{Vde} = \xi \frac{V_3^2}{2g} \tag{A19}$$

where the diffusion loss coefficient ξ is determined by the equivalent expansion angle of the nozzle θ_d. The angle is calculated by:

$$\theta_d = 2\tan^{-1}\left(\frac{D_9 - D_8}{2L_{89}}\right) \tag{A20}$$

The mixing loss behind the impeller is assumed to be the loss due to a sudden expansion of the meridional flow and a shearing effect between the flow exiting the impeller and that in the volute in the circumferential direction. The mixing loss behind the impeller is calculated by:

$$h_{ie} = \frac{[1 - b_2/b_3]^2 V_{m2}^2 + (V_{u2} - V_3)^2}{2g} \tag{A21}$$

where the first term was proposed in [20].

The skin friction factor λ in Eqs. (A4), (A11), (A16) is determined by the Reynolds number Re

and the equivalent sand roughness of wetted surfaces k_s. When the Reynolds number is $Re \le 2300$, the flow in a straight circular pipe is laminar regime, and the skin friction factor λ is determined theoretically by the formula [21]:

$$\lambda = \frac{64}{Re} \tag{A22}$$

where $Re = Re_i$ $(Re_i = W\, D_{hi}/\nu)$ for the impeller, $Re = Re_V$ $(Re_V = V_3\, D_{hV}/\nu)$ for the volute, but $Re = Re_d$ $(Re_d = V_{89}\, D_{99}/\nu)$ for the discharge nozzle are held.

When the Reynolds number is Re >2300, the boundary layer flow of the liquid in the impeller or volute or discharge nozzle is in turbulent regimes. If $k_s/\delta \le 1$ is held, where δ is the thickness of the sub-laminar layer, $\delta = 14.1\left(D_h/Re\sqrt{\lambda}\right)$, then the flow is in the turbulent hydraulically smooth regime and the friction factor λ depends on the Reynolds number Re (Re_i or Re_V or Re_d) rather than the relative roughness k_s/D_h (k_{si}/D_{hi} or k_{sV}/D_{hV} or k_{s89}/D_{89}), and is written as [21]:

$$\frac{1}{\sqrt{\lambda}} = 2.0\,\lg\left(Re\sqrt{\lambda}\right) - 0.8 \tag{A23}$$

The equivalent sand roughness of wetted surfaces is $k_s = 4.2Ra$ for cast walls with paint [22], Ra is the arithmetic average deviation of the rough surface valleys and peaks. The Ra values inside and outside impeller, inside volute and discharge nozzle are listed in Table 1.

If $1 < k_s/\delta \le 14$ is true, the boundary layer flow is in turbulent transitional or smooth regime and the friction factor λ is determined by both Re and k_s/D_h, and written as [21]:

$$\frac{1}{\sqrt{\lambda}} = 1.74 - 2\,\lg\left(\frac{2k_s}{D_h} + \frac{18.7}{Re\sqrt{\lambda}}\right) \tag{A24}$$

Finally, if $k_s/\delta > 14$, the flow is in the turbulent hydraulically rough regime, the factor λ is related to k_s/D_h only, and given by [21]:

$$\lambda = \frac{1}{\left(1.74 - 2\lg\frac{2k_s}{D_h}\right)^2} \tag{A25}$$

The coefficient ξ in Eqs. (9) and (19) for the diffusion loss is assumed to be equal to the coefficient for the diffusion loss in a conical diffuser apparently. The following empirical formula is obtained by best fitting the experimental data of the diffusion loss coefficient in the conical diffuser with fully developed inlet flow in [20]:

$$\xi = \begin{cases} \xi_0 & Re \ge 4\times10^5 \\ \xi_0 + 0.0131\ln(4\times10^5/Re) & Re < 4\times10^5 \end{cases} \tag{A26}$$

where $\xi_0 = -2\times10^{-7}\theta^4 + 4\times10^{-5}\theta^3 - 2.9\times10^{-3}\theta^2 + 0.1096\theta$-0.586, θ=θ_i for the impeller, θ=θ_d for the discharge nozzle. The last term in the second formula is based on the experimental data in [23].

The hydraulic loss in the pump h is the sum of all the losses in the impeller and volute, and reads as:

$$h = h_{if} + h_{id} + h_{ie} + h_{Vf} + h_{Vdf} + h_{Vde} \tag{A27}$$

A2 Leakage flow model

Two streams of the liquid are leaked to the impeller inlet from two side chambers through the clearance in the front and rear wear-rings and the balance holes on the hub as shown in Fig. A1a, respectively. The leakage flow rate determined by the pressure drops and flow coefficients across the two clearances. The pressure drops across the clearances in the front and rear wear-rings are expressed as:

$$\begin{cases} H_{wf} = H - \frac{V_3^2}{2g} - \omega_{ff}^2 \frac{R_2^2 - R_{wf}^2}{2g} \\ H_{wr} = H - \frac{V_3^2}{2g} - \omega_{fr}^2 \frac{R_2^2 - R_{wr}^2}{2g} \end{cases} \tag{A28}$$

where H_{wf} and H_{wr} are the pressure drops across the two clearances, R_{wf} and R_{wr} are the radii of the front and rear wear-rings, ω_{ff} and ω_{fr} are the mean rotating angular velocities of the liquid in the front and rear side chambers, respectively. ω_{ff} and ω_{fr} are calculated by the following formulas:

$$\begin{cases} \omega_{ff} = \kappa_f \omega \\ \omega_{fr} = \kappa_r \omega \end{cases} \tag{A29}$$

where κ_f and κ_r are the dimensionless mean rotating angular velocity coefficients of the liquid in the two side chambers. κ_f and κ_r are decided by the formulas [24, 25]:

$$\begin{cases} \kappa_f = \frac{1}{1+\left(\frac{R_{cf}}{R_2}\right)^2 \sqrt{\left(\frac{R_{cf}}{R_2}+5\frac{t_{cf}}{R_2}\right)\frac{C_{fcf}}{C_{fif}}}} \\ \kappa_r = \frac{1}{1+\left(\frac{R_{cr}}{R_2}\right)^2 \sqrt{\left(\frac{R_{cr}}{R_2}+5\frac{t_{cr}}{R_2}\right)\frac{C_{fcr}}{C_{fir}}}} \end{cases} \tag{A30}$$

where R_{cf} and R_{cr} are the radii of the pump casing in the front and rear side chambers to accommodate the impeller, R_{cf}=R_{cr}=R_2; t_{cf} and t_{cr} are the distances between the volute side walls and the side walls of the front and rear side chambers, see Fig. A2, t_{cf}=t_{cr}=0 here; C_{fcf} and C_{fif} are the mean skin friction factors on the side wall of the casing and outside surface of the impeller in the front side chamber; C_{fcr} and C_{fir} are the mean skin friction factors on the side wall of the casing and outside surface of the impeller in the rear side chamber. Based on the mean skin friction factor for laminar and turbulent boundary layers over a flat plate, C_{fcf}, C_{fcr}, C_{fif} and C_{fir} are calculated by the following empirical expressions [24, 25]:

$$\begin{cases} C_{fcf} = C_{fcr} = C_{fif} = C_{fir} = \frac{2.65}{Re_2^{0.875}} - \frac{2}{8Re_2+0.016/Re_2} + \frac{1.328}{\sqrt{Re_2}},\ Re_2 \le Re_{cr} \\ C_{fcf} = \frac{0.136}{\left[-\lg\left(0.2\frac{k_{scf}}{R_2}+\frac{12.5}{Re_2}\right)\right]^{2.15}}, C_{fcr} = \frac{0.136}{\left[-\lg\left(0.2\frac{k_{scr}}{R_2}+\frac{12.5}{Re_2}\right)\right]^{2.15}},\ Re_2 > Re_{cr} \\ C_{fif} = \frac{0.136}{\left[-\lg\left(0.2\frac{k_{sif}}{R_2}+\frac{12.5}{Re_2}\right)\right]^{2.15}}, C_{fir} = \frac{0.136}{\left[-\lg\left(0.2\frac{k_{sir}}{R_2}+\frac{12.5}{Re_2}\right)\right]^{2.15}},\ Re_2 > Re_{cr} \end{cases} \tag{A31}$$

where Re_{cr} is the critical Reynolds number at which the laminar boundary layer transitions to turbulent boundary layer, or vice versa; Re_{cr}=$3 \times 10^6/(1+10^4 T_u^{1.7})$ [26], T_u is the turbulent intensity of boundary layer, T_u=0.05 is a reasonable value for the flow in centrifugal pumps, thus Re_{cr}=48068; Re_2 is the impeller Reynolds number, Re_2=$R_2 u_2/\nu$; the formula at $Re_2 \leq Re_{cr}$ is from [26], and the formula at $Re_2 > Re_{cr}$ is after [24, 25].

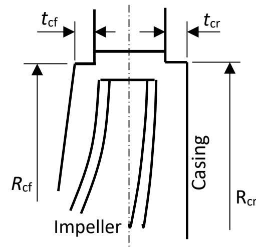

Fig. A2 Dimensions R_{cf}, R_{cr}, t_{cf} and t_{cr} of the pump casing

The clearances of the front and rear wear-rings are b_{wf}=b_{wr}=0.25mm, and the ratio of the balance hole cross-sectional area to the rear war-ring cross-sectional area is 3.2. Under these conditions the effect of the five balance holes on the leakage flow rate across the rear wear-ring is negligible [27]. Thus, the flow resistance generated by the balance holes should not considered. The leakage flow rates through the front and rear wear-rings are written as [27]:

$$\begin{cases} q_f = \frac{F_{wf}}{\sqrt{1.5+\lambda_{wf}\frac{l_{wf}}{2b_{wf}}}}\sqrt{2gH_{wf}} \\ q_r = \frac{F_{wr}}{\sqrt{1.5+\lambda_{wr}\frac{l_{wr}}{2b_{wr}}}}\sqrt{2gH_{wr}} \end{cases} \tag{A32}$$

where q_f and q_r are the leakage flow rates through the clearances in the front and rear wear-rings; the total leakage flow rate is q=q_f+q_r; F_{wf} and F_{wr} are the cross-sectional areas of the clearances in the front and rear wear-rings, F_{wf}=$\pi D_{wf} b_{wf}$, F_{wr}=$\pi D_{wr} b_{wr}$; λ_{wf} and λ_{wr} are the skin friction factors of the liquid flow through the clearances, and calculated by using the following empirical formulas [28]:

$$\begin{cases} \lambda_{wf} = \frac{48}{Re_{wf}},\ Re_{wf} \leq Re_{wfc} \\ \lambda_{wf} = \frac{0.2704}{Re_{wf}^{0.25}}\left[1+0.5\left(\frac{u_{wf}}{V_{mf}}\right)^2\right]^{3/8},\ Re_{wf} \leq Re_{wfc} \end{cases} \tag{A33}$$

and

$$\begin{cases} \lambda_{wr} = \frac{48}{Re_{wr}},\ Re_{wr} \leq Re_{wrc} \\ \lambda_{wr} = \frac{0.2704}{Re_{wr}^{0.25}}\left[1+0.5\left(\frac{u_{wr}}{V_{mr}}\right)^2\right]^{3/8},\ Re_{wr} \leq Re_{wrc} \end{cases} \tag{A34}$$

where u_{wf} and u_{wr} are the front and rear wear-rings rotational speed, u_{wf}=$R_{wf}\omega$, u_{wr}=$R_{wr}\omega$; V_{mf} and V_{mr} are the meridional velocities in the clearances in the front and rear wear-rings,

V_{mf}=q_f/F_{wf}, V_{mr}=q_r/F_{wr}; Re_{wf} and Re_{wr} are the Reynolds numbers of the clearances in the front and rear wear-rings, $Re_{wf}=b_{wf}V_{mf}/\nu$, $Re_{wr}=b_{wr}V_{mr}/\nu$; Re_{wfc} and Re_{wrc} are the critical Reynolds numbers that determine flow regimes in the clearances and calculated by [28]:

$$\begin{cases} Re_{wfc} = 996.6\left[1+0.5\left(\frac{u_{wf}}{V_{mf}}\right)^2\right]^{-1/2} \\ Re_{wrc} = 996.6\left[1+0.5\left(\frac{u_{wr}}{V_{mr}}\right)^2\right]^{-1/2} \end{cases} \tag{A35}$$

A3 Disc friction loss model

The disc friction power losses on outside surfaces of the impeller are calculated by the following equations:

$$\begin{cases} P_{mf} = \frac{1}{2}C_{Mf}f_{geo}f_{Lf}\rho\omega^3\left(R_2^5 - R_{wf}^5\right) \\ P_{mr} = \frac{1}{2}C_{Mr}f_{geo}f_{Lr}\rho\omega^3\left(R_2^5 - R_{wr}^5\right) \end{cases} \tag{A36}$$

where C_{Mf} and C_{Mr} are the torque coefficients on the impeller shroud (front surface) and hub (rear surface); f_{geo} is the shape factor for closed shape impellers of centrifugal pump, f_{geo}=1.22 [24, 25]; f_{Lf} and f_{Lr} are the leakage flow rate influencing factor on torque coefficients, and expressed by [24]:

$$\begin{cases} f_{Lf} = \exp\left[-\frac{300q_f}{\pi R_2^3\omega}\left(\frac{R_2}{R_{wf}}-1\right)\right] \\ f_{Lr} = \exp\left[-\frac{300q_r}{\pi R_2^3\omega}\left(\frac{R_2}{R_{wr}}-1\right)\right] \end{cases} \tag{A37}$$

There is the critical equivalent sand roughness at which C_{Mf} and C_{Mr} are dependent on wetted surface roughness and flow Reynolds number. The critical equivalent sand roughness on the impeller shroud and hub is given by [21]:

$$\begin{cases} k_{sifc} = \frac{100\nu}{\omega_f R_2} \\ k_{sirc} = \frac{100\nu}{\omega_r R_2} \end{cases} \tag{A38}$$

where k_{sifc} and k_{sirc} are the critical equivalent sand roughness on the impeller shroud and hub. If the equivalent sand roughness on the impeller shroud and hub k_{siof}, k_{sior} are smaller than k_{sifc} and k_{sirc}, then the C_{Mf} and C_{Mr} are as a function of Re_2, and expressed as [21]:

$$C_{Mf} = \begin{cases} 0.5\times 2\pi\frac{R_2}{t_f Re_2},\ Re_2 \le 2\times 10^4 \\ 0.5\times 2.67/\sqrt{Re_2},\ 2\times 10^4 < Re_2 \le 3\times 10^5 \\ 0.5\times 0.0622/Re_2^{0.2},\ Re_2 > 2\times 10^5 \end{cases} \tag{A39}$$

and

$$C_{Mr} = \begin{cases} 0.5\times 2\pi\frac{R_2}{t_r Re_2},\ Re_2 \le 2\times 10^4 \\ 0.5\times 2.67/\sqrt{Re_2},\ 2\times 10^4 < Re_2 \le 3\times 10^5 \\ 0.5\times 0.0622/Re_2^{0.2},\ Re_2 > 2\times 10^5 \end{cases} \tag{A40}$$

If k_{sif}, k_{sir} are larger than k_{sifc} and k_{sirc}, then the C_{Mf} and C_{Mr} are expressed by Re_2,

k_{sif} and k_{sir}, i.e. [29]:

$$\begin{cases} C_{Mf} = 0.5\left(\frac{k_{sif}}{R_2}\right)^{0.25}\left(\frac{t_f}{R_2}\right)^{0.1}\left(\frac{b_3}{t_f}\right)^{0.2} Re_2^{-0.2} \\ C_{Mr} = 0.5\left(\frac{k_{sir}}{R_2}\right)^{0.25}\left(\frac{t_r}{R_2}\right)^{0.1}\left(\frac{b_3}{t_r}\right)^{0.2} Re_2^{-0.2} \end{cases} \tag{A41}$$

The total disc friction power loss is the sum of the losses on the impeller shroud and hub, and expressed by:

$$p_m = 1.75\left(p_{mf} + p_{mr}\right) \tag{A42}$$

where the coefficient 1.75 is employed to consider the effect of real situation of flow in the side chambers on the disc friction power loss and the friction power losses in the shaft seals and bearings. The torque coefficient given by the empirical formulas based on experimental data of rotational disc in a cylindrical casing is always smaller than the torque coefficient of disc rotating with blade-like structures in a pump casing [30].

The above hydraulic, volumetric and disc friction loss models are coupled each other, these losses are calculated in an iteration manner in a composed MATLAB program. It was shown that the losses and three efficiencies no longer varied after 10 iterations.

References

[1] Liu M, Tan L, Cao S, Theoretical model of energy performance prediction and BEP determination for centrifugal pump as turbine, Energy, 2019, 172: 712-732.

[2] Lin T, Zhu Z, Li X, Li J, Lin Y, Theoretical, experimental, and numerical methods to predict the best efficiency point of centrifugal pump as turbine, Renewable Energy, 2021, 168: 31-44.

[3] Liu H, Tan M, Yuan S, Calculation of disk friction loss of centrifugal pumps, Transact ions of the CSAE, 2006, 22 (12): 107-109.

[4] Xiaoqi Jia, Yong Zhang, Hao Lv, et al. Study on external performance and internal flow characteristics in a centrifugal pump under different degrees of cavitation, Physics of Fluids.2023.DOI: 10.1063/5.0133377.

[5] Liu Z, Chen X, Wang D, Hou Y, Experiment and analysis of balance hole liquid leakage in centrifugal pump, Transactions of the CSAE, 2017, 33(7): 67-74.

[6] Derakhshan S, Nourbakhsh A, Theoretical, numerical and experimental investigation of centrifugal pumps in reverse operation, Experimental Thermal and Fluid Science, 2008, 32:1620-1627.

[7] Li X, Gao P, Zhu Z, Li Y, Effect of the blade loading distribution on hydrodynamic performance of a centrifugal pump with cylindrical blades, Journal of Mechanical Science and Technology, 2018, 32(3): 1161-1170.

[8] Qi B, Zhang D, Geng L, Zhao R, van Esch B P M, Numerical and experimental investigations on inflow loss in the energy recovery turbines with back-curved and front-curved impeller based on the entropy generation theory, Energy, 2022, 239:122426.

[9] Lai F, Huang M, Wu X, Nie C, Li G, Local entropy generation analysis for cavitation flow within a centrifugal pump, Journal of Fluids Engineering, 2022, 144:101206.

[10] Jia X, Zhang Y, Lv H, Zhu Z, Study on external performance and internal flow characteristics in a centrifugal pump under different degrees of cavitation, Physics of Fluids, 2023, 35: 014104..

[11] Yuan Y, Fang Y, Tang L, Effects of non-uniform elbow inflow on the unsteady flow and energy development characteristics of a centrifugal pump, Physics of Fluids, 2023, 35: 015152.

[12] Kan K, Zhao F, Xu H, Feng J, Chen H, Liu W, Energy performance evaluation of an axial-flow pump as turbine under conventional and reverse operating modes based on an energy loss intensity model, Physics of Fluids, 2023, 35: 015125.

[13] Stepanoff A J, Centrifugal and Axial Flow Pumps (2nd Edition), New York: John Wiley & Sons, 1957.

[14] Yang J, Zhang R, Research on the efficiency of centrifugal pump, Fluid Machinery, 2002, 30(10): 25-27.

[15] Li, W G, Su, F Z, Xiao C, Experimental investigations of performance of a commercial centrifugal oil pump, Journal of Fluids Engineering, 2002, 124(2): 554-557

[16] Li W G, Influence of the number of impeller blades on the performance of centrifugal oil pumps, World Pumps, 2002, 427: 32-35.

[17] Li W G, Blade exit angle effects on performance of a standard industrial centrifugal oil pump, Journal of Applied Fluid Mechanics, 2011, 4(3): 105-119.

[18] Kabele W, A practical approach to centrifugal pump design, SAE Transactions, 1971, 80(3): 1750-1759

[19] Wiesner F J, A review of slip factors for centrifugal impellers, Journal of Engineering for Power, 1967, 89(4): 558-572.

[20] White F M, Fluid Mechanics, New York: McGraw-Hill INC, 1994.

[21] Schlichting, H, Boundary-Layer Theory, New York: McGraw-Hill Company, 1968.

[22] Acharya M, Bornstein J and Escudier M P, Turbulent boundary layers on rough surfaces, Experiments in Fluids, 1986, 4: 33-47.

[23] Fried E and Idelchik I E, Flow Resistance: A Design Guide for Engineer. New York: Hemisphere Publishing Corporation, 1989.

[24] Gulich J F, Effect of Reynolds number and surface roughness on the efficiency of centrifugal pumps, Journal of Fluids Engineering, 2003, 125(4): 670-678.

[25] Gulich J F, Disk friction losses of closed turbomachine impellers, Forschung im Ingenieurwesen, 2003, 68(2): 87-95.

[26] Brauer H and Sucker D, Umströmung von Platten, Zylinder und Kugeln, Chemie Ingenieur Technik, 1976, 48(8): 665-736.

[27] Li W G, Model of flow in the side chambers of an industrial centrifugal pump for delivering viscous oil, Journal of fluids engineering, 2013, 135(5): 051201.

[28] Asanuma T, On the flow of liquid between parallel walls in relative motion, transactions of JSME, 1951, 17(60): 140–146.

[29] Nemdili A and Hellmann D H, Development of an empirical equation to predict the disc friction losses of a centrifugal pump, Proceedings of the 6th International Conference on Hydraulic Machinery and Hydrodynamics, Timisoara, Romania, October 21-22, 2004, 235-240.

[30] Nemdili A and Hellmann D H, Investigations on fluid friction of rotational disks with and without modified outlet sections in real centrifugal pump casings, on losses of a centrifugal pump, Forschung im Ingenieurwesen, 2007, 71(1): 59-67.

[31] Miloševic, M, Brkic D, Praks P, Litricin D, Stajic, Z, Hydraulic losses in systems of conduits with flow from laminar to fully turbulent: A new symbolic regression formulation, Axioms, 2022, 11, 198, https://doi.org/10.3390/axioms11050198.